JOURNAL OF APPLIED ELECTROCHEMISTRY 21 (1991) 543–551

Electrooxidation/electroreduction processes at composite iron hydroxide layers in carbonate-bicarbonate buffers

E. B. CASTRO, J. R. VILCHE

Instituto de Investigaciones Fisicoquímicas Teóricas y Aplicadas (INIFTA), Facultad de Ciencias Exactas, Universidad Nacional de la Plata. Sucursal 4, Casilla de Correo 16, (1900) La Plata, Argentina

Received 13 March 1990; revised 8 November 1990

The electrooxidation/electroreduction processes at precipitated iron hydroxide layers on platinum electrodes have been studied in carbonate-bicarbonate buffers at 25° C by using electrochemical methods. The initial characteristics and properties of the hydrous iron hydroxide were changed by varying the precipitation conditions of the chemically formed active materials. Different potential-time perturbation programs were employed to analyse the contribution of redox couples within the composite iron hydroxide layers on platinum electrodes and the corresponding electrochemical responses were compared with results obtained for massive iron electrodes in the same solutions. The complex electroreduction and electrooxidation processes are discussed on the basis of a reaction model which takes into account the incorporation of $FeCO_3$ in the hydrous iron hydroxide layer and its oxidation to FeOOH species, which in turn can participate in electroreduction reactions yielding Fe_3O_4, $Fe(OH)_2$, and soluble Fe(II) species.

1. Introduction

The characteristics and properties of oxide layers and corrosion scales formed on iron and low alloy steels are remarkably dependent on the chemical composition of the aqueous media in which the metal surface is exposed [1, 2]. The ability to identify compounds present on corroded metal surfaces [3–8] and to determine the participation of these surface species in oxidation/reduction reactions, should facilitate the understanding of processes involved in metal dissolution and passivation [9, 10]. The oxidation and reduction of iron oxides take place during the corrosion of iron and steel surfaces exposed to the atmosphere, as well as to air-saturated waters, due to the change between wet and dry periods for the first case [11, 12] and between flow and stagnation conditions for the second case [10]. In both environments the hydrous iron oxide-hydroxide layer system participates in oxidation/reduction cycles which strongly influence the base metal corrosion process. Accordingly, reduced iron oxide scales which can be re-oxidized further, contribute to the non-steady state behaviour of the metallic iron dissolution [1, 12].

Redox processes involving iron hydroxide layers have been extensively investigated in the last decade, particularly for different types of oxides and oxy-hydroxides in contact with iron electrodes in alkaline solutions [13–20]. Oxide layer structure interpretations are mostly in agreement with duplex or multiple layer structures whose water content and composition depend on its formation conditions [4, 5, 17]. To overcome the interference of the proper iron dissolution reaction, electrochemical studies have been also carried out by using iron hydroxide layer electrodes prepared on conducting substrates [21–26] which proved to be inactive in the potential range where the oxidation and reduction processes of the active material occur. In this respect, chemically precipitated hydrous iron hydroxide layers on platinum electrodes have been employed to analyse the voltammetric behaviour in strongly alkaline aqueous media [26, 27] and lend themselves satisfactorily for the investigations of the properties of such active materials and of their interactions with the solution constituents.

Previous works [28–31] on the electrodissolution and passivation of polycrystalline Fe electrodes in neutral aqueous solutions concluded that the presence of bicarbonate ions in the electrolyte favours instability phenomena at the outer part of the prepassive layer where the interaction between Fe^{2+} and HCO_3^- ions plays an important role. Aqueous solutions containing carbonate and bicarbonate ions are commonly found in any absorbing carbon dioxide system. Apparently, two distinct passivating layers can exist in these solutions, the more stable layer formed at high positive potentials probably consists essentially of a Fe(III)-oxide, whereas at relatively more negative potentials a hydrous lower oxide whose stability depends on the bicarbonate ion concentration, was found [30–36]. The susceptibility of low carbon steels to stress corrosion cracking [37–40] and corrosion fatigue [41, 42] in those solutions was well established.

0021-891X/91 $03.00 + .12

The present paper will illustrate the role of precipitated hydrous iron hydroxide layers in the study of the dissolution and passivation of iron in carbonate/bicarbonate buffers. It will be shown that the new developments resulting in the preparation of well defined active material layers make it possible to elucidate various questions related to surface processes responsible for the formation and reduction of iron corrosion products.

2. Experimental

The experimental setup was the same as described in previous publications [23, 26, 27]. The working electrodes consisted of chemically precipitated iron hydroxide layers on platinum wire ("Specpure", Johnson Matthey Chemicals Ltd, 0.5 mm diameter, 0.24 cm^2 apparent area), which was previously cleaned by immersion in a 1:1 H_2SO_4 + HNO_3 mixture for 15 min and later thoroughly rinsed in three-fold distilled water. The precipitation of the active material layers was made by alternate and repetitive immersing of the substrate in 0.01 M $FeSO_4$ solution and in either 0.01 M KOH (Electrode A) or 0.75 M $KHCO_3$ (Electrode B) solution. The immersion time in each solution was set at 5 s and the number of alternate immersions (N) was varied from 5 up to 100. Immediately after the electrode preparation, it was dipped into the 0.75 M $KHCO_3$ + 0.05 M K_2CO_3 solution at 25°C, pH 8.9, in the measurement cell under purified nitrogen gas saturation, and polarised for a time τ_0 at different initial potentials, E_i, before the voltammetric run. For comparison, some measurements were also performed with both high purity polycrystalline iron electrodes and chemically precipitated iron hydroxide layers on massive iron electrodes.

The precipitating and the electrolyte solutions were prepared from analytical grade (p.a. Merck) reagents and three-fold distilled water. Potentials were measured against a SCE, provided with a Luggin capillary tip and properly shielded to avoid chloride ion diffusion, but in the text they are referred to the NHE scale. The perturbing potential programs (E/t) applied between preset cathodic ($E_{s,c}$) and anodic ($E_{s,a}$) switching potentials to the working electrode are indicated in each figure. The iron concentration in the precipitated layer was determined by atomic absorption spectrometry [27, 43].

3. Results

Reference voltammograms for masive iron electrodes in quiescent 0.75 M $KHCO_3$ + 0.05 M K_2CO_3 were recorded at $v = 0.025\,V\,s^{-1}$ (Fig. 1, full curve) and $0.0025\,V\,s^{-1}$ (Fig. 1, dashed curve) between $E_{s,c} = -0.96$ V and $E_{s,a} = 0.34$ V to identify the different anodic as well as cathodic current contributions and their corresponding potential ranges. In the positive going potential sweep, the iron dissolution peaks (I and II) at approx. −0.60 V and −0.45 V corresponding to the formation of the prepassive and

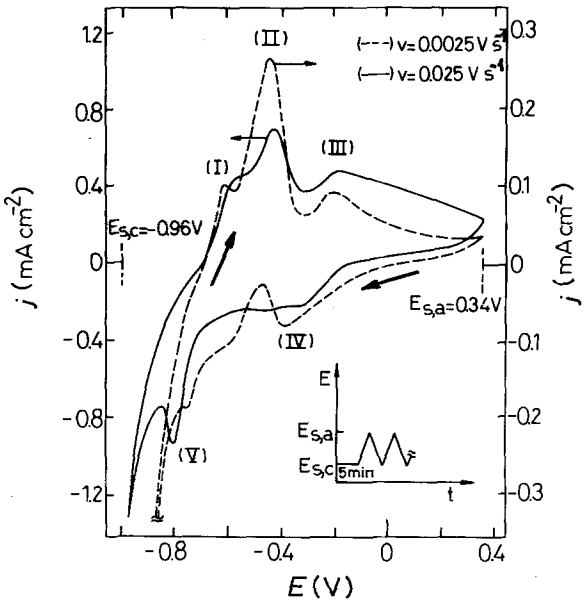

Fig. 1. Influence of v on voltammograms obtained with an iron electrode in still 0.75 M $KHCO_3$ + 0.05 M K_2CO_3 between $E_{s,c} = -0.96$ V and $E_{s,a} = 0.34$ V. $v = 0.0025\,V\,s^{-1}$ (dashed curve); $v = 0.025\,V\,s^{-1}$ (full curve).

passive films, respectively, are followed by a broad anodic peak (III) at approx. −0.2 V. In the reverse sweep, two cathodic peaks (IV and V) at about −0.4 V and −0.8 V can be observed, although the latter appears strongly overlapped to the HER current contribution. The voltammetric charge involved in peak I, $Q_{p,I} = 1.9 \pm 0.3\,mC\,cm^{-3}$, is practically independent of v, pH, and concentration of HCO_3^- ions, at least for $c_{HCO_3^-} < 0.25$ M [35]. On the other hand, as the height of peak II becomes independent of v for $v \leqslant 0.0025\,V\,s^{-1}$ it can be assumed that the metal dissolution process in the potential range of peak II occurs under quasi-steady conditions [44]. According to previous works [30, 31] under stirring (not shown here) peak III disappears whereas the iron dissolution peak II increases considerably and a reactivation of the metal electrodissolution process at approximately −0.5 V during the reverse sweep was noticed. This reactivation effect for the anodic reaction takes place at potentials more negative than cathodic peak IV [30, 31]. The influence of the cathodic and anodic switching potentials on the relative contribution of the different voltammetrically recorded peaks is given in Fig. 2. As $E_{s,c}$ is increased stepwise the charge involved in the anodic peaks diminishes (Fig. 2a), whereas as $E_{s,a}$ is fixed at more negative potentials the anodic reactivation contribution during the negative going potential excursions increases (Fig. 2b). Apparently, there is a close relationship between the reactions associated with peaks I and V.

The reference voltammograms for platinum electrodes run at different v values between $E_{s,c} = -0.51$ V and different $E_{s,a}$ have shown the already known electrosorption/electrodesorption of both hydrogen and oxygen, their corresponding potential regions separated by a narrow *d.l.* charging/discharging potential range at about −0.1 V. When $E_{s,c}$ is fixed below −0.55 V, where the net HER from water dis-

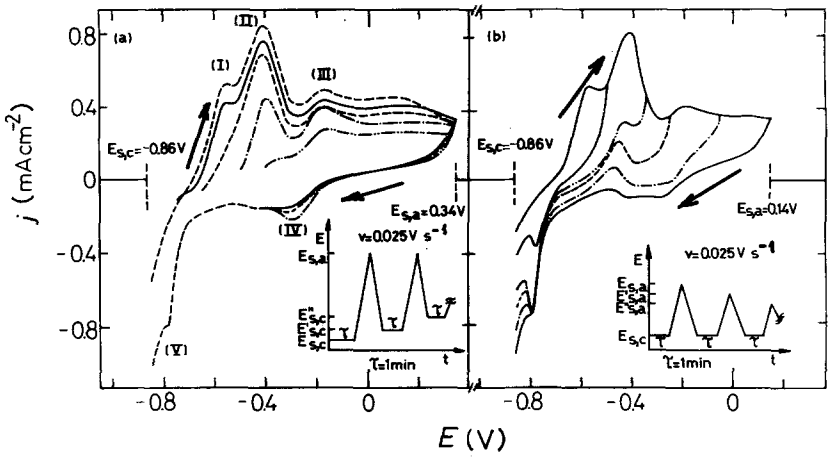

Fig. 2. Influence of the cathodic (a) and anodic (b) switching potentials on the voltammograms obtained with an iron electrode in still 0.75 M $KHCO_3$ + 0.05 M K_2CO_3 at $v = 0.025\,V\,s^{-1}$. The perturbing potential program is indicated in the figure. $\tau = 1$ min.

charge takes place, and the potential is held at $E_{s,c}$ a certain time τ before a single potential cycle, a new anodic peak is observed at approx. -0.52 V during the positive going potential scan (Fig. 3). This anodic current contribution is obviously associated with the electrooxidation of H_2, which was previously electroformed at the relatively high negative potentials. It is interesting to note that the current density reached at the anodic peak at about -0.52 V for a voltammogram run at $v = 0.1\,V\,s^{-1}$ including a holding time $\tau = 5$ min at $E_{s,c} = -0.66$ V, is in the order of $17\,mA\,cm^{-2}$ whereas that recorded when $E_{s,c} = -0.51$ V diminishes to a value of approximately $0.04\,mA\,cm^{-2}$ (Fig. 3).

The voltammetric response of the chemically formed hydrous iron hydroxide layers precipitated on platinum electrodes depends on the precipitation conditions and on the perturbing potential program, although at $v \geqslant 0.1\,V\,s^{-1}$ it is practically independent of the alternate immersions number for N values between 20 and 100. It is worth noting that for freshly prepared electrodes the amount of precipitated iron hydroxide evaluated through atomic absorption spectroscopy increases almost linearly with N (Fig. 4).

Apparently from Fig. 4 the amount of Fe-species precipitated in one alternate immersion corresponds to $\partial m_{Fe}/\partial N = 1.6 \pm 0.1\,\mu g\text{-Fe}\,cm^{-2}$, a value which might be associated with a theoretical charge in the order of $2.7\,mC\,cm^{-2}$ for a $1\,e^-$ electrochemical redox reaction. Fig. 5 shows up the influence of $E_{s,a}$ on voltammograms run at $v = 0.025\,V\,s^{-1}$ with an electrode A for $N = 100$. The current peak multiplicity exhibits, in principle, the electrochemical characteristics of massive iron electrodes, but in the case of precipitated iron hydroxide electrodes the voltammetric charge of peak II is smaller and an anodic hump at approximately 0.1 V is observed. The anodic charge involved up to the peak potential of current peak I, which can be assigned to the first electrooxidation stage of Fe [29, 30, 45], is in the order of about $1\,mC\,cm^{-2}$ for massive iron and approximately $1.4\,mC\,cm^{-2}$ for precipitated iron hydroxide electrodes. Furthermore, the absence of current contributions due to either formation or electrooxidation of molecular hydrogen at the platinum base suggests that the precipitated iron hydroxide layer and its electroreduction products at high negative $E_{s,c}$ values have

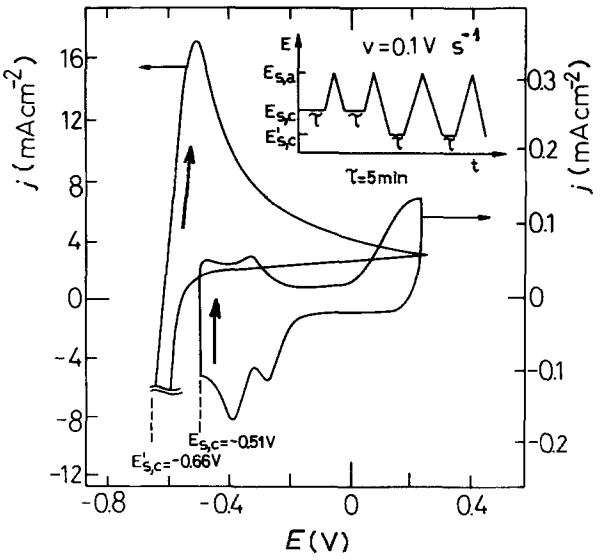

Fig. 3. Voltammograms obtained with a platinum electrode at $v = 0.1\,V\,s^{-1}$ between $E_{s,c} = -0.66$ V and $E_{s,a} = 0.2$ V and between $E'_{s,c} = -0.51$ V and $E_{s,a} = 0.2$ V after holding at either $E_{s,c}$ or $E'_{s,c}$ during $\tau = 5$ min before each potential cycle.

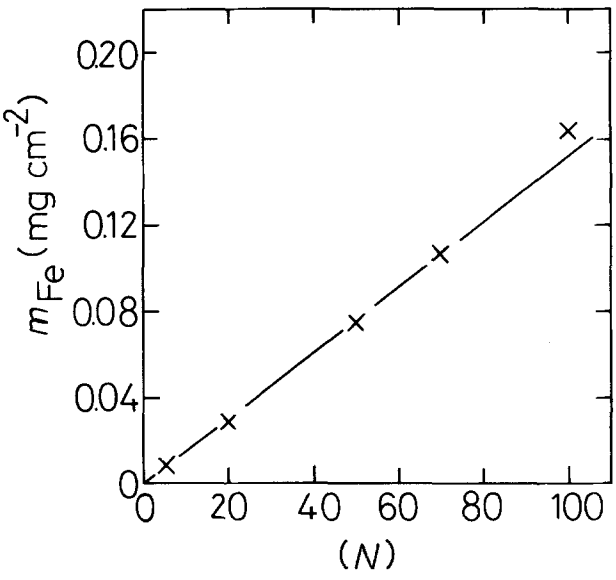

Fig. 4. Dependence of N in the preparation procedure of precipitated iron hydroxide electrode A on m_{Fe}, as evaluated by atomic absorption spectroscopy.

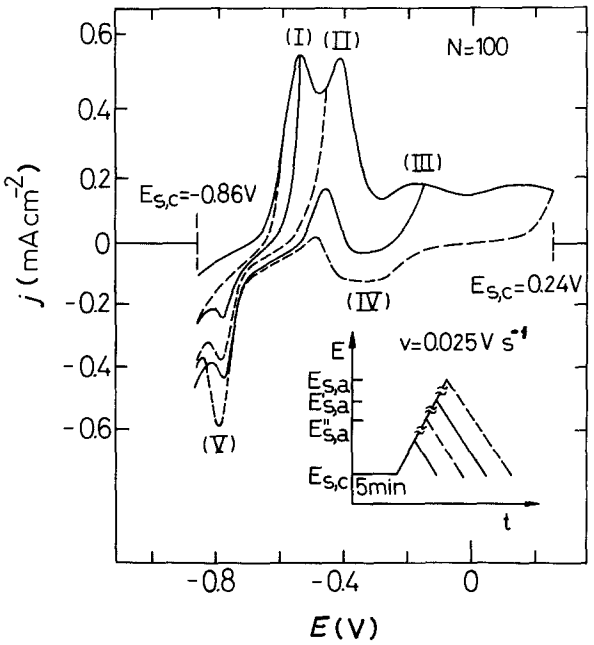

Fig. 5. Influence of $E_{s,a}$ on voltammograms obtained with a precipitated iron hydroxide electrode A on Pt, at $v = 0.025\,V\,s^{-1}$ from $E_{s,c} = -0.86\,V$ after holding at $E_{s,c}$ during 5 min. $N = 100$.

covered completely the Pt substrate. The whole anodic voltammetric charge reaches about $9\,mC\,cm^{-2}$.

The dependence of the N value used in the precipitated iron hydroxide electrode preparation procedure on voltammograms performed at $v = 0.1\,V\,s^{-1}$ (Fig. 6a) and $v = 0.025\,V\,s^{-1}$ (Fig. 6b) after a previous cathodisation at $E_{s,c} = -0.86\,V$, reveals that the characteristics of the different current contributions are very similar for $N = 50$ and $N = 100$, whereas the voltammetric charge turns gradually to diminish for $N \leqslant 20$ being this effect enhanced as v decreases. Otherwise, the relative contribution of peak II becomes better defined with increasing N and decreasing v values (Fig. 6).

For thin iron hydroxide layers ($N = 5$) the voltammetric charge in the potential range of peaks I and II recorded after a cathodisation at $E_{s,c} = -0.86\,V$ during a time τ, increases only slightly according to τ for $\tau \leqslant 10$ min and decreases progressively for $\tau > 10$ min (Fig. 7). This effect can be clearly observed at low v, whereas at $v \geqslant 0.1\,V\,s^{-1}$ the voltammetric charge becomes apparently independent of τ. On the other hand, for thick iron hydroxide layers (i.e. $N \geqslant 50$) the anodic charge decreases during potential cycling, but as a prolonged intermediate cathodisation at a potential value more negative than that of peak V is included the voltammogram subsequently run exhibits the same anodic behaviour of that recorded for the initial potential scan (Fig. 8). Thus, when a sufficiently long holding time at $E_{s,c} = -0.86\,V$ is set either after running 16 potential cycles (Fig. 8a) or between each triangular potential scan (Fig. 8b), the following voltammogram resembles the first one obtained with the freshly prepared electrode. It should be noticed that with an electrode A prepared by employing $N = 20$, the voltammetric charge diminishes gradually even when an intermediate cathodisation at $E_{s,c}$ for $\tau = 10$ min between each successive potential cycle is included, whereas in the case of thinner precipitated layers ($N = 5$) the typical electrochemical response of the Pt substrate is reached after a few potential cycles. From these results one can conclude that the potentiodynamic behaviour of the precipitated active material is mainly determined by the electroreduction level of the iron-containing surface species according to the $E_{s,c}$ and τ values. Likewise, thin iron hydroxide layers can be dissolved yielding a soluble complex containing bicarbonate ion and Fe(II) species, probably $FeHCO_3^+$ [31, 44].

When the voltammograms were performed by using a freshly prepared iron hydroxide electrode A which was previously anodised at $E_{s,a} = 0.24\,V$ for a certain time τ_0 (Fig. 9). The electroreduction of the surface active material involves four cathodic current contributions (A, A', B, and C) preceeding the HER region. The current contributions A/A' and C are located in the potential range of peaks IV and V, respectively, and the current contribution B at approximately $-0.71\,V$ seems to be a new peak. The whole cathodic charge increases according to τ_0, although

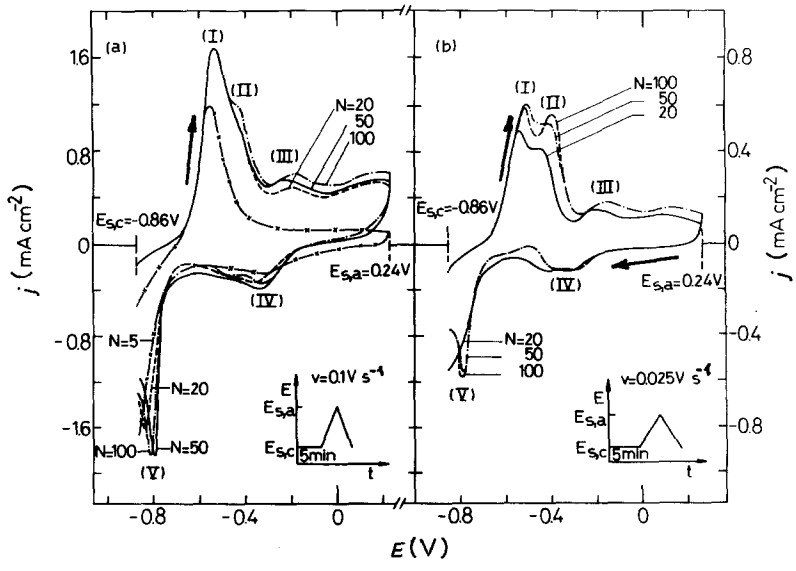

Fig. 6. Influence of N in the preparation procedure of precipitated iron hydroxide electrode A on voltammograms obtained between $E_{s,c} = -0.86\,V$ and $E_{s,a} = 0.24\,V$ at (a) $v = 0.1\,V\,s^{-1}$ and (b) $v = 0.025\,V\,s^{-1}$.

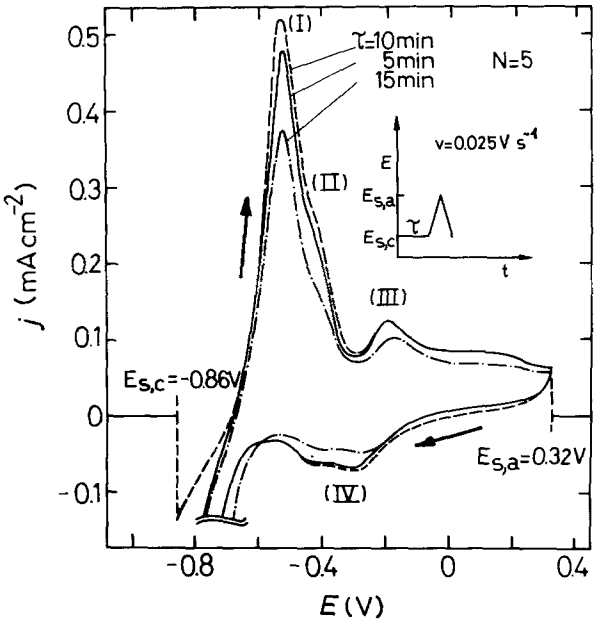

Fig. 7. Influence of the holding time τ at $E_{s,c} = -0.86\,V$ on voltammograms obtained with a precipitated iron hydroxide electrode A on Pt at $v = 0.025\,V\,s^{-1}$ between $E_{s,c}$ and $E_{s,a} = 0.32\,V$. $N = 5$.

the j/E profile remains qualitatively unaltered. During the subsequent positive potential going scan run from $E_{s,c} = -0.86\,V$ (Fig. 9a), anodic peaks I and III are clearly observed. Otherwise, measurements carried out by including an intermediate cathodization at $E_{s,c}$ in the net HER region during a time $\tau = 1\,min$ (Fig. 9b) show up the typical three anodic current peaks I, II, and III corresponding to the active-to-passive transition of iron electrodes [29, 34, 36]. The relative charge contribution of peak II increases as $E_{s,c}$ is set more negatively and also as τ increases.

To gain further information about the different iron-containing surface species and on their electrooxidation/electroreduction levels the precipitated iron hydroxide electrode B was employed. According to its preparation procedure the active material of electrode B on Pt consists of a mixture of hydrous iron hydroxide and hydrous iron carbonate species. A typical voltammogram run with electrode B at $v = 0.025\,V\,s^{-1}$ between $E_{s,c} = -0.86\,V$ and $E_{s,a} = 0.34\,V$, starting after a cathodisation at $E_{s,c}$ during 5 min, is shown in Fig. 10. Under these circumstances, the electrode B prepared by using $N = 20$ exhibits a potentiodynamic response similar to that obtained with a massive iron electrode (see Fig. 2a), although for the latter the charge of peak II is greater than that recorded with electrode B under the same experimental conditions. However, in respect to the total electrooxidation/electroreduction charge there is clear differences between the active material of precipitated iron hydroxide electrodes B (Fig. 10) and A (Figs. 5 and 6b). For electrode B, the relative contribution of peak II is greater and that of peak I lower in comparison to those data obtained by using electrode A. Moreover, when the voltammetric measurement is preceded by a potential holding at $E_{s,a} = 0.24\,V$ for $\tau_0 = 30\,s$, the voltammograms obtained at $v = 0.025\,V\,s^{-1}$ between $E_{s,a}$ and $E_{s,c} = -0.86\,V$ for electrodes B (Fig. 11a) and A (Fig. 11b) formed by using $N = 20$, differ remarkably in their charge distribution. For electrode B the charge involved in both cathodic peak A and anodic peak III becomes greater and the difference between their peak potentials smaller than those values resulting for electrode A under comparable experimental conditions (Fig. 11). It is interesting to note that for an electrode B the voltammetric response of anodised iron hydroxide layers after a potential holding for 2 min at $E_i = -0.25\,V$ set in the peak A′ potential range, the current contributions of peaks A′ and A disappear and the charge involved in peak B is enhanced in comparison to that determined from voltammogram shown in Fig. 11b.

Similar effects appear also in voltammograms run between $E_{s,c} = -0.66\,V$ and $E_{s,a} = 0.24\,V$ after a previous cathodisation at $E_{s,c}$, being this potential value more positive than that required to produce Fe(0) in the electroreduction process and accordingly, peak I and II are not observed (Fig. 12). These results clearly indicate the participation of iron carbonate

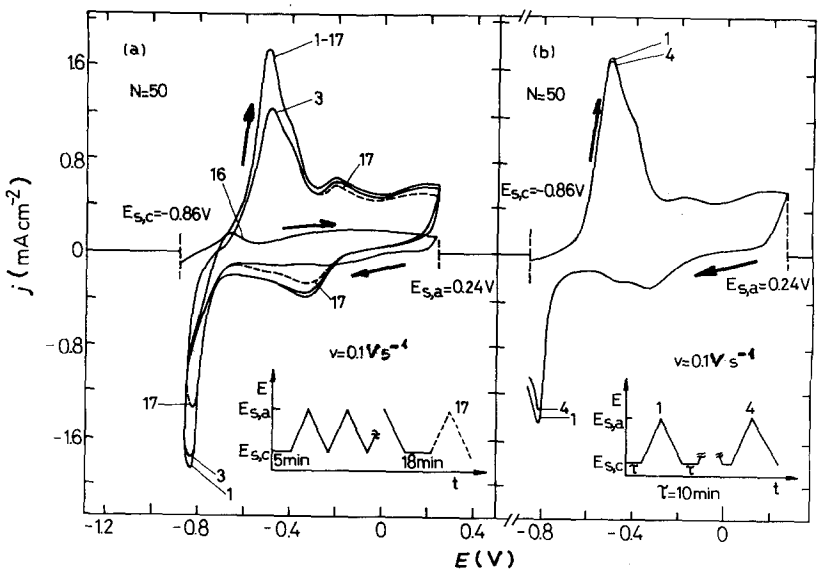

Fig. 8. Voltammograms obtained with a precipitated iron hydroxide electrode A at $v = 0.1\,V\,s^{-1}$ between $E_{s,c} = -0.86\,V$ and $E_{s,a} = 0.24\,V$. (a) Repetitive potential cycling combined with a potential holding at $E_{s,c}$ during 18 min before the 17th potential cycle; (b) repetitive potential cycling combined with potential steps at $E_{s,c}$ during 10 min before each potential cycle. $N = 50$.

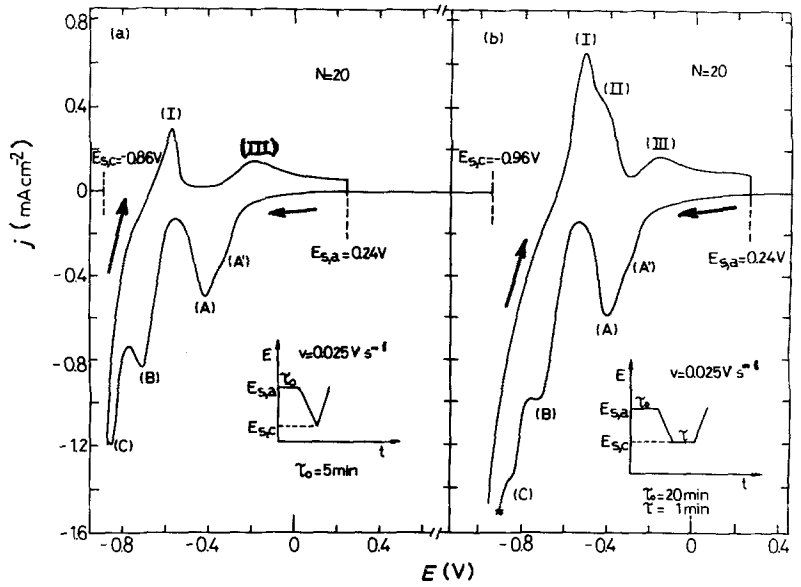

Fig. 9. Voltammograms obtained with a precipitated iron hydroxide electrode A at $v = 0.025\,V\,s^{-1}$ starting after a previous anodisation at $E_{s,a} = 0.24\,V$ during a time τ_0. The E/t perturbation programs are shown in the figures. (a) $\tau_0 = 5\,min$, $E_{s,c} = -0.86\,V$; (b) $\tau_0 = 20\,min$, $E_{s,c} = -0.96\,V$, and a holding time at $E_{s,c}$ during $\tau = 1\,min$. $N = 20$.

species in the redox reactions associated with the complex conjugated peaks either III/A or III/IV, as the corresponding peak assignment depends only on the perturbing potential program.

4. Discussion

The electrochemical behaviour of the iron hydroxide electrode on platinum can be interpreted by considering the properties of the precipitated active material layers, in comparison with results obtained by using massive iron electrodes under comparable experimental conditions. The iron hydroxide layer on platinum formed through chemical precipitation involves initially a hydrous mixtures of $Fe(OH)_2$ and $Fe(OH)_3$ species in the case of electrode A, whereas the coprecipitation of $FeCO_3$ is also implied for electrode B.

In situ optical data provided by using ellipsometry [5, 46], Raman spectroscopy [34], Fourier transform IR-spectroscopy [47], and XPS and ISS examinations of surface layers with a specimen transfer in a closed system [48] agree in the assignment of the first oxidation level of iron to the formation of a thin non-protective hydrous $Fe(OH)_2$ layer in the potential range of peak I. According to recent electrochemical

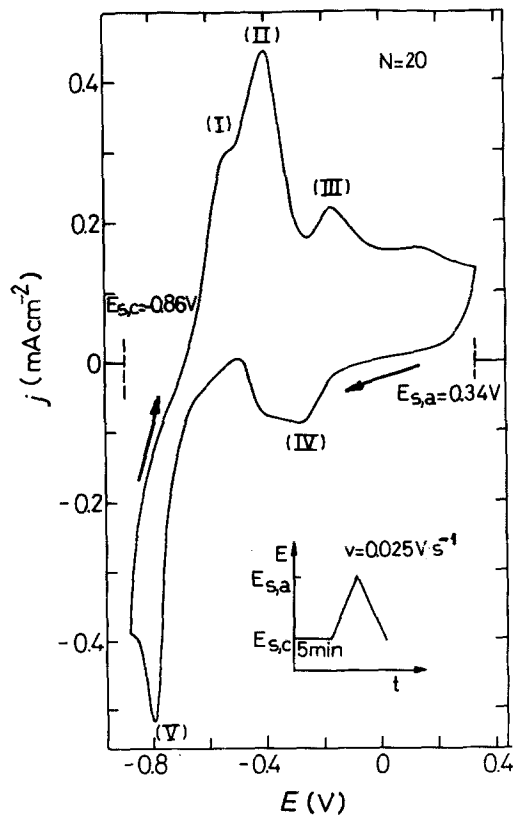

Fig. 10. Voltammogram obtained with a precipitated iron hydroxide electrode B at $v = 0.025\,V\,s^{-1}$ between $E_{s,c} = -0.86\,V$ and $E_{s,a} = 0.34\,V$. $N = 20$.

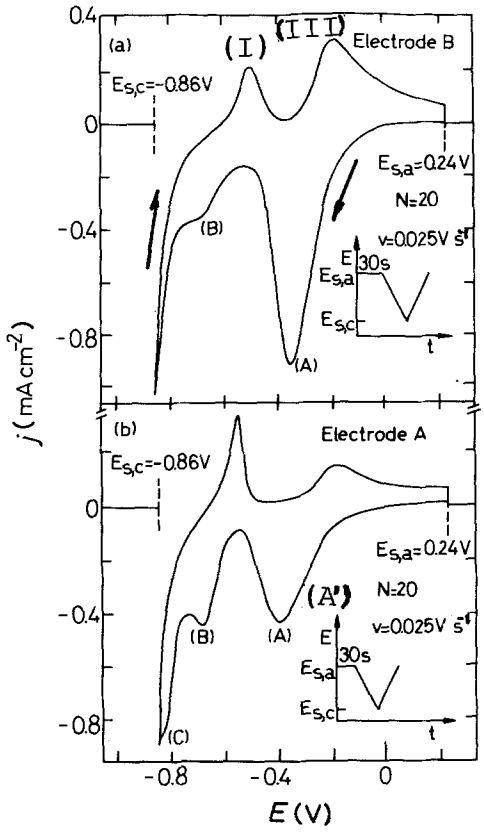

Fig. 11. Voltammograms obtained with precipitated iron hydroxide electrodes B (a) and A (b) at $v = 0.025\,V\,s^{-1}$ between $E_{s,a} = 0.24\,V$ and $E_{s,c} = -0.86\,V$ after a previous anodisation at $E_{s,a}$ during 30 s. $N = 20$.

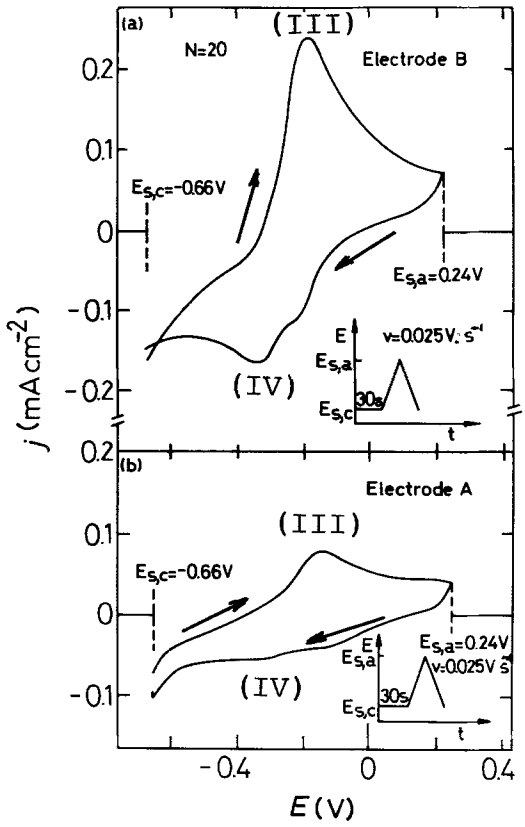

Fig. 12. Voltammograms obtained with precipitated iron hydroxide electrodes B (a) and A (b) at $v = 0.025\,V\,s^{-1}$ between $E_{s,a} = -0.66\,V$ and $E_{s,a} = 0.24\,V$ after a previous cathodisation at $E_{s,c}$ during 30 s. $N = 20$.

impedance spectroscopy [49] and RRDE [44] data of the iron dissolution and passivation in carbonate/bicarbonate buffers the formation of soluble compounds containing Fe(II) and HCO_3^-, probably $FeHCO_3^+$ or $Fe(HCO_3)_2$, becomes the major contribution in the potential region of peak II. The RRDE results indicated that the concentrations of soluble Fe(II) species largely exceeds those expected under saturation conditions with either $Fe(OH)_2$ or $FeCO_3$. At potentials close to $E_{p,II}$ the growth of Fe_3O_4 as a constituent of the inner part of the passive layer takes place [5, 17, 50, 51], whereas XPS results showed that carbonate species appears in the composition of the outer part of the anodic layer formed in still solutions [43, 44]. From previous voltammetric studies covering a wide range of experimental conditions [28–31], it is clear that the surface anodic products related to peaks I and II can be electroreduced in the potential range of peak V (see, for instance, Fig. 2b).

When $E_{s,c}$ is set at potential values corresponding to peak V or more negatively, voltammograms resulting for thick active layers ($N \geqslant 50$) chemically precipitated on Pt electrodes exhibit a distribution of anodic and cathodic peaks (Figs. 5 and 6b) which coincides with the typical electrochemical behaviour of massive iron [30, 31] (see Figs. 1 and 2). This fact is useful to draw qualitative conclusions regarding the formation of Fe(O) from a reaction such as:

$$Fe(OH)_2 + 2e^- \rightleftharpoons Fe(0) + 2OH^- \qquad (1)$$

The equilibrium potential of Reaction 1 at pH 8.9 is about -0.67 V [52, 53]. For precipitated hydrous iron hydroxide layers formed on Pt according to the preparation procedure of electrode B, at high negative potentials the electroreduction of $FeCO_3$ to Fe(O) through the global reaction

$$FeCO_3 + 2e^- \rightleftharpoons Fe(0) + CO_3^{2-} \qquad (2)$$

cannot be disregarded. It should be noted that the reduction of iron oxides to metallic iron in strongly alkaline media at high cathodic polarisation has been studied *in situ* by Mössbauer spectroscopy [16] and second harmonic generation [54].

At a relatively fast potential sweep rate, i.e. $v = 0.1\,V\,s^{-1}$ (Fig. 8), a prolonged intermediate cathodisation at high negative $E_{s,c}$ values is required in order to record again the initial voltammetric profile. This result suggests that the electroreduction of iron oxides occurs through the formation of a thin reduced layer containing Fe(0) and Fe(II) species with the simultaneous generation of soluble Fe(II) species. The latter can be incorporated in the porous structure of the hydrous outer layer in the case of precipitated iron hydroxide electrodes formed by employing $N \geqslant 20$ in their preparation procedure. According to ellipsometric and RRDE data for iron in carbonate-bicarbonate solution [33], as at the end of the cathodic reduction there is a sudden decrease in thickness accompanied by an abrupt release of Fe(II) ions, this can be taken as evidence that the oxide layer is reduced *in situ* from the inside out.

As far as the precipitated iron hydroxide layer covers the Pt substrate (uniformly) the HER takes place on the electroreduced products of the active material, which in turn consist mainly of a thin Fe(0) layer beneath the remaining hydrous iron hydroxide outer layer. The amount of Fe-containing species increases according to N (Fig. 4). Otherwise, the thickness of the cathodically formed Fe(0) layer reaches only a few monolayers, as can be clearly seen by comparison of voltammograms obtained with a precipitated iron hydroxide layer prepared by employing $N = 100$ (Fig. 5) and a massive Fe electrode (Fig. 2a). On the other hand, for thin precipitated iron hydroxide layers the current contribution of the Fe(0) electrooxidation in the potential range of the peak II diminishes remarkably (Fig. 7). The porous structure of the hydrous iron hydroxide outer layer can be envisaged from the peak potential values which are practically coincident with the location of peak potentials in voltammograms run with massive Fe electrodes. This turns out to be important in dealing with the pH value of the electrolyte solution at the surface of the electroreduced species of the hydrous iron hydroxide at the inner part of the composite active material layer. Recently, a comparative electrochemical and ellipsometric study of polycrystalline iron in different alkaline solutions [55] indicated that the initial $Fe(OH)_2$ formation at the inner part of the passive layer level is only slightly influenced by either the cation or the presence of Cl^- ions in solution, in

contrast to their large effect at the outer part of the hydrous passive layer where the Fe(II)/Fe(III) redox reactions take place.

Voltammograms obtained with hydrous iron hydroxide layers on Pt electrodes (Figs 5, 6, and 10) reveal that the electrooxidation/electroreduction processes occurring in the potential range of the complex conjugated peaks III/IV (or III/A–A′) appears to be the same as already reported for massive Fe in still carbonate-bicarbonate solutions [29, 30]. Furthermore, according to voltammograms obtained with electrodes B and A, both after anodising in the passive region (Fig. 11) and after cathodising at potentials just more positive than −0.7 V to avoid the formation of Fe(0) (Fig. 12), peak III can be associated with the electrooxidation of $FeCO_3$ to Fe(III)-containing oxide species. The corresponding reactions can be stated as

$$FeCO_3 + 2H_2O \rightleftharpoons \alpha\text{-}FeOOH + CO_3^{2-} + 3H^+ + e^- \quad (3a)$$

$$FeCO_3 + 2H_2O \rightleftharpoons \gamma\text{-}FeOOH + CO_3^{2-} + 3H^+ + e^- \quad (3b)$$

$$FeCO_3 + 3H_2O \rightleftharpoons Fe(OH)_3 + CO_3^{2-} + 3H^+ + e^- \quad (3c)$$

At pH 8.9 and $c_{CO_3^{2-}} = 0.05$ M the equilibrium potentials of Reactions 3a and 3b lie close to −0.231 V and −0.072 V, respectively, and that corresponding to Reaction 3c is about 0.040 V [53, 56]. These data indicate that the contribution of Reaction 3c can be disregarded in the potential range of peak III, although it can probably be related to the small anodic hump observed at approximately 0.1 V.

At potentials more negative than peak IV, the electroreduction of the Fe(III)-containing oxide species initially yields $Fe(OH)_2$ through a reaction which can be represented as

$$\text{hydrous [FeOOH or } Fe(OH)_3] + H^+ + e^- \rightleftharpoons \text{hydrous [FeOH . OH]} \quad (4)$$

Accordingly, during the reduction of Fe(III)-species described by Equation 4, the parallel formation of Fe_3O_4 can also occur through

$$2\,[FeOOH] + [Fe(OH)_2] \rightleftharpoons [Fe_3O_4] + 2H_2O \quad (5)$$

$$3\,[FeOOH] + H^+ + e^- \rightleftharpoons [Fe_3O_4] + 2H_2O \quad (6)$$

$$2\,[FeOOH] + Fe^{2+}(aq) \rightleftharpoons [Fe_3O_4] + 2H^+(aq) \quad (7)$$

For anodised iron hydroxide electrodes (Figs 9 and 11) Fe_3O_4 formed at the inner part of the hydrous iron hydroxide layer can be reduced in the potential range of peak B according to

$$Fe_3O_4 + H_2O + 2H^+ + 2e^- \rightleftharpoons 3\,Fe(OH)_2 \quad (8)$$

whose equilibrium potential at pH 8.9 is about −0.72 V [52, 53]. Furthermore, in the porous hydrous oxide layer structure the ionic equilibria involving Fe^{2+}, OH^-, HCO_3^-, CO_3^{2-}, and $FeHCO_3^+$ ions should be considered [31, 35]. Likewise, the role of the anions on the composition and morphology of different model colloidal corrosion products has been clearly stressed as the stability and dissolution rate of these particles are strictly related to the adsorption of the ligand material on the metal hydrous oxide [57, 58].

High resolution electron microscope examinations revealed that thin polymeric films act as precursors in the precipitation of iron oxides [59]. One can conclude that the first stage involves the iron ion hydrolysis leading to a polymeric iron hydroxide layer by way of hydroxide bridges. As this type of oxide-hydroxide gel-like structures should have a significant ion exchange capacity, the OH^- groups may be partially replaced by HCO_3^-. The nature of the HCO_3^- complexity ability to Fe(II) ions can be also derived from RRDE data [44]. The tendency to incorporate a relatively large amount of water in the porous outer layer structure allows the comparison between the electrochemical behaviour of chemically precipitated iron hydroxide layers on Pt electrodes with that obtained for anodically formed iron oxide-hydroxide layers on Fe. Therefore, it is reasonable that the inner part of the porous hydrous oxide layer is likely to behave according to the electrolyte solution composition. On the other hand, voltammograms obtained after anodising of the surface active material (Figs 9 and 11) are in accordance with an increase of the number of oxo-bridges in respect to hydroxo-bridges in the polymeric iron hydroxide layer.

The model presented in this work based on the electrochemical response of hydrous iron hydroxide layer can be compared with results corresponding to iron oxide scales and with processes involved in the phenomenological behaviour of rusting. It is well known that the rate of HER on a mill-scaled steel surface in carbonate-bicarbonate solutions is affected by the different forms of metallic Fe as it depends strongly on the electrical history of the interface [60]. Some unusual cathodic polarisation characteristics of carbon steel in neutral aqueous media reported in CO_2 saturated environments were attributed to anion changes in the diffuse double layer and partly to the reduction of magnetite and carbonate to the base metal [61]. The presence of $FeCO_3$ and its participation in reactions of this type of cathodically protected mill-scaled steel surface can be postulated even at high negative potentials. By radiotracer methods both reversible and irreversible adsorption of C-containing species on an iron electrodeposited electrode in CO_2-saturated neutral electrolyte were identified [62]. The irreversible adsorption can be interpreted as resulting mainly from carbonate ion incorporation in the passive layer. Consequently it may be expected that the inhibition of iron corrosion due to carbonate ion is only effective in alkaline solutions where the bicarbonate ion concentration still

has low values. This means that the stability of a passivating layer on iron or low alloy carbon steels in CO_2-saturated unbuffered waters at relatively low potentials should depend on the local pH. With increasing potential hydrous ferrous surface species are oxidised to a more anhydrous Fe(III)-oxide species and the inner barrier layer thickness diminishing the ferrous ion diffusion into solution. According to recent RRDE data [44] no contribution of Fe(II) was detected for iron at high positive potentials in carbonate-bicarbonate buffers.

Acknowledgement

This research project was financially supported by the Consejo Nacional de Investigaciones Científicas y Técnicas and the Comisión de Investigaciones Científicas de la Provincia de Buenos Aires.

References

[1] R. W. Staehle and H. Okuda (eds), 'Passivity and its Breakdown on Iron and Iron Base Alloys', NACE, Houston (1976).
[2] R. P. Frankenthal and J. Kruger (eds), 'Passivity of Metals', The Electrochemical Society, Princeton (1978).
[3] N. C. Debnath and A. B. Anderson, *J. Electrochem. Soc.* **129** (1982) 2169.
[4] K. Ogura, A. Fujishima, Y. Nagae and K. Honda, *J. Electroanal. Chem.* **162** (1986) 241.
[5] O. A. Albani, J. O. Zerbino, J. R. Vilche and A. J. Arvia, *Electrochim. Acta* **31** (1986) 1403.
[6] R. Goetz, D. F. Mitchell, B. MacDougall and M. Y. Graham, *J. Electrochem. Soc.* **134** (1987) 535.
[7] J. O'M. Bockris, *Corros. Sci.* **29** (1989) 291.
[8] G. Larramona and C. Gutiérrez, *J. Electrochem. Soc.* **136** (1989) 2171.
[9] M. Stratmann, K. Bohnenkamp and H. J. Engell, *Corros. Sci.* **23** (1983) 969.
[10] A. Kuch, *ibid.* **28** (1988) 221.
[11] H. Schwitter and H. Böhni, *J. Electrochem. Soc.* **127** (1980) 15.
[12] H. Kaesche, 'Metallic Corrosion', NACE, Houston (1985).
[13] R. S. Schrebler Guzmán, J. R. Vilche and A. J. Arvia, *Electrochim. Acta* **24** (1979) 395.
[14] J. Dünnwald and A. Otto, *Z. Anal. Chem.* **319** (1984) 738.
[15] L. D. Burke and M. E. G. Lyons, *J. Electroanal. Chem.* **198** (1986) 347.
[16] C. Fierro, R. E. Carbonio, D. Scherson and E. B. Yeager, *J. Phys. Chem.* **91** (1987) 6579.
[17] S. Juanto, J. O. Zerbino, M. I. Miguez, J. R. Vilche and A. J. Arvia, *Electrochim. Acta* **32** (1987) 1743.
[18] S. Haupt and H. H. Strehblow, *Langmuir* **3** (1987) 873.
[19] J. Y. Zou and D. T. Chin, *Electrochim. Acta* **33** (1988) 477.
[20] N. Boucherit, P. Delichere, S. Joiret and A. Hugot-Le Goff, *Materials Science Forum* **44/45** (1989) 51.
[21] J. M. Lecuire, *J. Electroanal. Chem.* **66** (1975) 195.
[22] L. Formaro, *Corros. Sci.* **20** (1980) 1251.
[23] V. A. Macagno, J. R. Vilche and A. J. Arvia, *J. Appl. Electrochem.* **11** (1981) 417.
[24] Y. Tamaura, C. Kameshima and T. Katsura, *J. Electrochem. Soc.* **128** (1981) 1447.
[25] J. W. Schultze, S. Mohr and M. M. Lohrengel, *J. Electroanal. Chem.* **154** (1983) 57.
[26] M. E. Vela, J. R. Vilche and A. J. Arvia, *Electrochim. Acta* **31** (1986) 1633.
[27] M. C. Galindo, M. E. Martins, J. R. Vilche and A. J. Arvia, *J. Appl. Electrochem.* **20** (1990) 102.
[28] C. R. Valentini, C. A. Moina, J. R. Vilche and A. J. Arvia, *Anal. Asoc. Quím. Arg.* **71** (1983) 555.
[29] M. E. Vela, J. R. Vilche and A. J. Arvia, in 'Passivity of Metals and Semiconductors' (edited by M. Froment), Elsevier, Amsterdam (1983) pp. 59–63.
[30] C. R. Valentini, C. A. Moina, J. R. Vilche and A. J. Arvia, *Corros. Sci.* **25** (1985) 985.
[31] E. B. Castro, C. R. Valentini, C. A. Moina, J. R. Vilche and A. J. Arvia, *ibid.* **26** (1986) 781.
[32] G. T. Burstein and D. H. Davies, *ibid.* **20** (1980) 1143.
[33] P. Southworth, A. Hamnett, A. M. Riley and J. M. Sykes, *ibid.* **28** (1988) 1130.
[34] J. C. Rubin and J. Dünnwald, *J. Electroanal. Chem.* **258** (1989) 327.
[35] E. B. Castro, S. G. Real, S. B. Saidman, J. R. Vilche and R. H. Milocco, *Materials Science Forum* **44/45** (1989) 417.
[36] S. Zecevic, D. M. Drazic and S. Gojkovic, *J. Electroanal. Chem.* **265** (1989) 179.
[37] R. D. Armstrong and A. C. Coates, *Corros. Sci.* **16** (1976) 423.
[38] E. Wendler-Kalsch, *ibid.* **23** (1983) 601.
[39] R. N. Parkins, C. S. O'Dell and R. R. Fessler, *ibid.* **24** (1984) 343.
[40] J. A. Might and D. J. Duquette, in 'Critical Issues in Reducing the Corrosion of Steels' (edited by H. Leidheiser and S. Haruyama), NACE, Houston (1986) pp. 3–16.
[41] R. H. Ricci, L. B. Berardo, L. M. Gassa and J. R. Vilche, Proc. 9th Intern. Congr. Met. Corros., Vol. 3, pp. 161–78, National Research Council of Canada, Toronto (1984).
[42] E. B. Castro, L. M. Gassa and J. R. Vilche, Proc. 10th Intern. Congr. Met. Corros., Vol. 3, Oxford & Ibh Publ., Madras (1987) pp. 2071–80.
[43] E. B. Castro, Ph.D. Thesis, University of La Plata (1989).
[44] E. B. Castro, J. R. Vilche and A. J. Arvia, *Corros. Sci.* **32** (1991) 37.
[45] M. E. Vela, J. R. Vilche and A. J. Arvia, *J. Appl. Electrochem.* **16** (1986) 490.
[46] V. Jovancicevic, R. Kainthla, Z. Tang, B. Yang and J. O'M. Bockris, in 'Surfaces, Inhibition, and Passivation' (edited by E. McCafferty and R. J. Brodd), The Electrochemical Society, Pennington (1986) pp. 192–209.
[47] N. Brinda-Konopik, H. Neugebauer, G. Gidaly and G. Nauer, *Mikrochim. Acta* **9** (1981) 329.
[48] S. Haupt, C. Calinski, U. Collisi, H. W. Hoppe, H. D. Speckmann and H. H. Strehblow, *Surf. Interf. Anal.* **9** (1986) 357.
[49] R. H. Milocco, E. B. Castro, S. G. Real and J. R. Vilche, in 'Transient Techniques in Corrosion Science and Engineering' (edited by W. H. Smyrl, D. D. Macdonald and W. J. Lorenz), The Electrochemical Society, Pennington (1989) pp. 88–100.
[50] Z. Q. Huang and J. L. Ord, *J. Electrochem. Soc.* **132** (1985) 24.
[51] S. Juanto, J. O. Zerbino, J. R. Vilche and A. J. Arvia, in 'Surfaces, Inhibition, and Passivation' (edited by E. McCafferty and R. J. Brood), pp. 226–38, The Electrochemical Society, Pennington (1986).
[52] M. Pourbaix, 'Atlas of Electrochemical Equilibria', Pergamon Press, Oxford (1966) p. 307.
[53] T. Misawa, *Corros. Sci.* **13** (1973) 659.
[54] B. M. Biwer, M. J. Pellin, M. W. Schauer and D. M. Gruen, *Langmuir* **4** (1988) 121.
[55] O. A. Albani, L. M. Gassa, J. O. Zerbino, J. R. Vilche and A. J. Arvia, *Electrochim. Acta* **35** (1990) 1437.
[56] J. G. Thomas, T. J. Nurse and R. Walker, *Br. Corros. J.* **5** (1970) 87.
[57] E. Kalman, T. Radnai, G. Palinkas, F. Hajdu and A. Vertes, *Electrochim. Acta* **33** (1988) 1223.
[58] E. Matijevic, *Corrosion* **35** (1979) 264.
[59] J. R. Fryer, A. M. Gildawie and R. Paterson, *Nature* **252** (1974) 574.
[60] R. N. Parkins, A. J. Markworth, J. H. Holbrock and R. R. Fressler, *Corrosion* **41** (1985) 389.
[61] G. I. Ogundele and W. E. White, *Corrosion* **42** (1986) 71.
[62] A. Wieckowski, E. Ghali, M. Szklarczyk and J. Sobkowski, *Electrochim. Acta* **28** (1983) 1627.